Journal of
Ceramic Science
and Technology

J. Ceram. Sci. Tech., 03 [02] 89-94 (2012)
DOI: 10.4416/JCST2012-00006
available online at: http://www.ceramic-science.com
© 2012 Göller Verlag

Thermal Oxidation of Sintered Silicon Carbide Used for Diesel Particulate Filter Walls

T. Thomé*[1], M. Capelle[1], L. Thomé[2], T. Prenant[1], M. Néret[1]

[1]PSA Peugeot Citroen, Centre Technique de Vélizy, DRD/DCHM/PMXP/TAC, Route de Gisy, 78943 Vélizy-Villacoublay, France
[2]Centre de Spectrométrie Nucléaire et de Spectrométrie de Masse (CSNSM), CNRS-IN2P3-Univ. Paris-Sud, Bât. 108, 91405 Orsay, France

received February 1, 2012; received in revised form March 20, 2012; accepted April 18, 2012

Abstract

The temperature dependence of the thermal oxidation of sintered silicon carbide (SiC) used for diesel particulate filter walls (DPF) is investigated. Silicon carbide samples are heated at temperatures between 770 K and 1470 K for different annealing times to study the effect of both the temperature and the duration on the oxidation kinetics. The thickness and composition of the oxide layers are characterized by means of XPS and RBS. Silicon oxycarbides (SiC_xO_y) are first formed and then silicon dioxide (SiO_2) appears above 770 K. Different types of SiO_2 layers can be identified. The compounds obtained depend on thermal oxidation conditions.

Keywords: SiC, SiO_2, thermal properties, oxycarbide, oxidation

I. Introduction

Diesel particulate filters (DPF) are devices widely used to remove particulate matter and soot formed as result of incomplete combustion from the exhaust gas of diesel engines. One of the most commonly employed materials for these filters is silicon carbide (SiC). A critical step (commonly called filter regeneration) necessary for the efficient operation of a DPF is to clean it in order to eliminate the accumulated particulates whenever the quantity of accumulated particles exceeds a certain amount. It involves heating up the filter to the soot combustion temperature. The crucial point is that, in some cases, failure and damage of the DPF can occur during this regeneration cycle. Actually, under extreme conditions, such as high temperature and humidity and low oxygen partial pressure, active oxidation can occur instead of passive oxidation, which leads to SiC consumption and then to DPF damage [1].

The thermal behaviour of SiC has been widely studied since this material is of great interest for many advanced products developed for energy and electronic devices, especially owing to its excellent properties at high temperature [2–4]. The oxidation of silicon carbide can follow two different mechanisms depending on the oxygen partial pressure and on the temperature and humidity [5–7]. At low temperature and humidity and at high oxygen partial pressure, mainly passive oxidation occurs. This behaviour leads to the formation of a silica protective layer that prevents the SiC surface from further oxidation, according to the reaction:

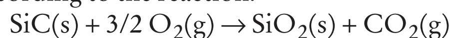

$SiC(s) + 3/2\ O_2(g) \rightarrow SiO_2(s) + CO_2(g)$

* Corresponding author: tristan.thome@mspa.com

At high temperature and humidity and at low oxygen partial pressure, active oxidation tends to takes place, so that SiO and CO gases are produced. This behaviour induces consumption of the SiC surface, since no protective silica layer is formed, according to the reaction:

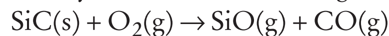

$SiC(s) + O_2(g) \rightarrow SiO(g) + CO(g)$

As most DPF working conditions are difficult to evaluate and to control, the thermal oxidation of sintered silicon carbide used for DPF walls was investigated in order to find the conditions to form a stable thin silica layer capable of resisting active oxidation. X-ray photoelectron spectroscopy (XPS) is a very convenient technique to determine both the thickness and composition of thin layers of oxides on SiC. For instance, XPS allows measurement of the depth profile of silicon oxides formed during various thermal treatments. Rutherford backscattering spectrometry (RBS) and scanning electron microscopy (SEM) were also used to measure thick layers of oxides and to check the evolution of the surface quality of SiC DPF walls after annealing.

II. Experimental

Samples (3 x 10 mm^2) were cut from DPF segments made of silicon carbide (R-SiC type). The raw materials used for the manufacture of the filter are commercial grades of silicon carbide together with organic binders and additives. First step is the mixing of the raw materials to form a plastic compound. The compound is then extruded into segments. Finally, the filter segments are sintered at 2470 K under argon in a high-temperature furnace. These segments correspond to as-received samples.

Then, samples were heated under air atmosphere at various temperatures from 770 to 1470 K (with equal heating and cooling rates of 10 K·min^{-1} and relative humidity between 30 and 40 %) for different annealing times in order to study the effect of both the temperature and the duration on the oxidation kinetics. One sample was weighed before and after annealing to detect possible weight gain resulting from the oxidation treatment, which could indicate a passive oxidation regime.

The changes in the structure and composition with the temperature of sintered silicon carbide surfaces were determined using a field emission gun (FEG) scanning electron microscope (JEOL-JSM-6340F) coupled with an energy-dispersive X-ray spectrometer (OXFORD-INCA Energy 350).

The thickness and composition of the oxide layers were characterized with RBS and XPS. RBS spectra were recorded with the ARAMIS accelerator of the CSNSM in Orsay. A 1.4 MeV He^+ beam was used and the silicon surface barrier detector was fixed at 165° relative to the incident beam to measure the RBS signal. The oxide layer thicknesses were determined from RBS spectra using the SIMNRA software [8] with specific Rutherford cross-sections.

XPS analyses were conducted with an AXIS ULTRA X-ray Photoelectron Spectrometer (Kratos Analytical, Manchester, UK), using monochromatic Al Kα radiation and operating at 10 kV and 10 mA. A take-off angle of 90° with respect to the sample surface was used. The area of analysis was 300 μm × 700 μm. The pressure in the chamber was around 2×10^{-9} mbar. To eliminate charging effects, the analyses were performed with a charge-compensating low-energy electron system. High-resolution C 1s, O 1s and Si 2p core level spectra were acquired at 10 eV pass energy. A least square fitting routine was then employed and the spectra were fitted with a sum of Gaussian-broadened Lorentzian line shape peaks, each one representing distinct chemical species. Before fitting, the background was removed by means of the Shirley's method [9].

III. Results and Discussion

Fig. 1 shows SEM images in a backscattered electron imaging (BEI) mode of a DPF sample before and after annealing at 1270 K for 2 h. The surface structure and composition of the SiC particles are similar. The average SiC particle size is around 12 μm. The main additives are concentrated on the SiC particle boundaries and are composed of vanadium, iron, titanium, nickel and aluminium (detected by means of SEM-EDX). No structural changes are observed up to 1470 K.

Fig. 2 presents XPS spectra of the Si 2p core levels of a DPF sample before and after annealing at 970 K for 30 min and at 1470 K for 2 h. Owing to electrostatic charging effects occurring on surfaces, especially for filters with thick silica layers, the C 1s peak corresponding to contaminant atmospheric carbon usually fixed at 285 eV is used to normalize the binding energies of the photoelectron peaks of the Si 2p core levels. The spectrum of the as-received filter can be fitted using two components at 100.1 and 101.7 eV, which can be attributed to SiC and silicon oxycarbide (SiC_xO_y), respectively [10–13]. The chemical shift (with the SiC peak) that corresponds to SiC_xO_y is generally taken between 1 and 2 eV, whereas that corresponding to SiO_2 varies from 2.5 to 3.5 eV depending on the type of silica that is formed [14–17]. Thus, no SiO_2 layer is formed on the silicon carbide walls of as-received filters. We can only observe the presence of a SiC_xO_y layer with a thickness of a few angstroms if we assume an inelastic mean free path (IMFP) of electrons in silicon oxide around 3 nm [18–19]. This IMFP value of 3 nm is used hereafter for all types of silicon oxides to determine the corresponding thicknesses from XPS spectra. A third component appears at 102.7 eV (energy shift of 2.6 eV) on the spectrum recorded on the filter annealed at 970 K for 30 min, which corresponds to SiO_2. Only a SiO_2 layer is observed on the spectrum recorded on the filter annealed at 1470 K for 2 h, which is characterized by an energy shift of 3.3 eV.

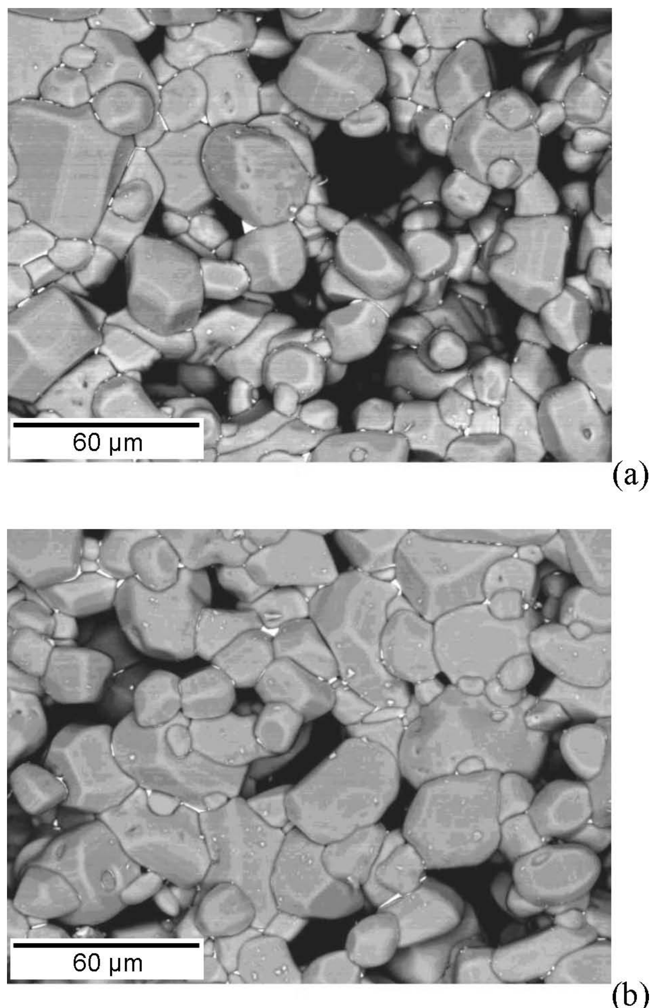

Fig. 1: SEM images in a backscattered electron imaging (BEI) mode of a DPF sample before (a) and after annealing at 1270 K for 2 h (b).

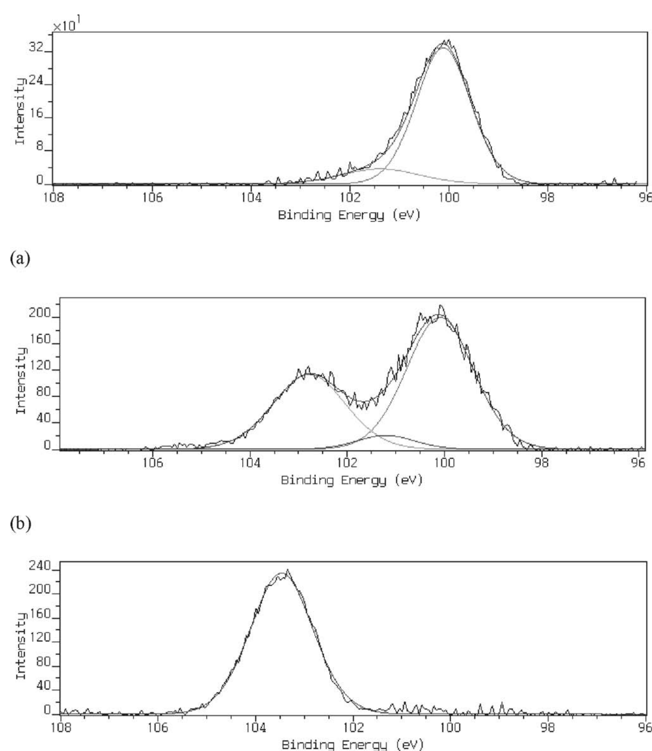

Fig. 2: XPS spectra after energy normalization of the Si 2p core levels of a DPF sample before (a) and after annealing at 970 K for 30 min (b) and 1470 K for 2 h (c).

XPS spectra of the Si 2p core levels of DPF are shown in Fig. 3 for different annealing temperatures up to 1470 K. The characteristics of the oxide layers which are calculated from these spectra are listed in Table 1. The thickness of silicon oxycarbide (SiC_xO_y) increases up to about 1 nm for an annealing at 770 K. Then silicon dioxide (SiO_2) appears between 770 and 970 K at the SiC/SiC_xO_y interface region. Two different XPS energy shifts corresponding to SiO_2 are observed depending on the conditions of thermal annealing. At high temperatures and annealing times, the energy shift is around 3.3 eV, whereas it is near 2.7 eV at the beginning of the SiO_2 formation. These two distinct values show that two different types of SiO_2 layers can grow on the SiC/SiC_xO_y surface depending on annealing conditions. Fig. 4 shows XPS spectra of the C 1s core levels of DPF annealed at different temperatures up to 1470 K. A shoulder or a small shift towards higher binding energies is observed on the component at 282 eV (corresponding to the SiC) for the samples annealed at 770, 970 and 1070 K, which confirms that a silicon oxycarbide (SiC_xO_y) is present on the SiC surface at 770 and 970 K and which indicates that the first SiO_2 formed at 1070 K is also likely to contain carbon.

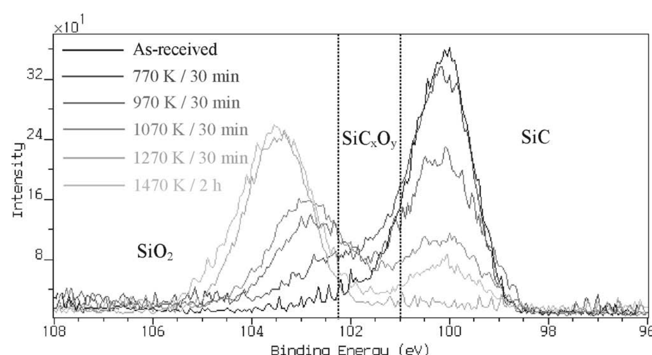

Fig. 3: XPS spectra after energy normalization of the Si 2p core levels of a DPF sample for different annealing temperatures up to 1470 K.

Table 1: Characteristics of oxide layers measured from RBS and XPS Si 2p spectra.

Samples	Oxide/SiC ratio (%)	Main oxide	Energy shift (eV) between SiC and the main oxide	Oxide layer thickness (nm)
As received	0.11	SiC_xO_y	1.6	0.4 (XPS)
770 K - 30 min	0.22	SiC_xO_y	2.0	0.7 (XPS)
970 K - 30 min	0.60	SiO_2	2.6	1.7 (XPS)
1070 K - 30 min	1.38	SiO_2	2.8	3.0 (XPS)
1270 K - 30 min	4.55	SiO_2	3.3	6.0 (XPS)
770 K - 2 h	0.21	SiC_xO_y	2.0	0.8 (XPS)
970 K - 2 h	1.00	SiO_2	2.7	2.5 (XPS)
970 K - 5 h	1.50	SiO_2	2.8	3.2 (XPS)
1270 K - 2 h	10.1	SiO_2	3.3	8.0 (XPS)
1370 K - 1h	-	SiO_2	3.3	40 (RBS)
1470 K - 2 h	-	SiO_2	3.3	260 (RBS)

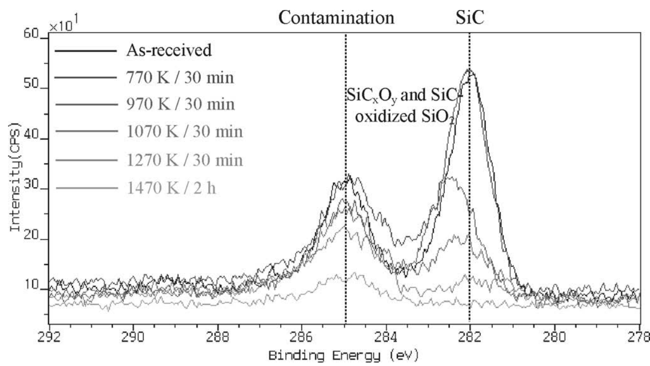

Fig. 4: XPS spectra after energy normalization of the C 1s core levels of a DPF sample for different annealing temperatures up to 1470 K.

The corresponding binding energies of the different components used to fit photoelectron peaks of the C 1s core levels are presented in Table 2. Only two components with energies of 282 eV (SiC) and 285 eV (carbon contamination) are observed for the as-received sample, which means that even if silicon oxycarbide (SiC_xO_y) is clearly detected analyzing Si 2p core level spectra, the layer is likely to be very thin (maximum of a few angstroms). A third component appears around 282.6 eV only between 770 and 1070 K, which confirms the formation of SiC_xO_y and of a non-pure SiO_2 that can be called SiC-oxidized SiO_2 [14] in this range of annealing temperatures. Surprisingly, a huge difference is observed between the Si 2p binding energies attributed to SiC_xO_y and SiC-oxidized SiO_2 (respectively 2 and around 2.7 eV for energy shifts, see Table 1) whereas there is almost no difference on C 1s binding energies (about 282.6 eV for both). Concerning the two different SiO_2 species, the fact that only two components with energies of 282 eV (SiC) and 285 eV (carbon contamination) are observed at 1270 K shows that a SiC-oxidized SiO_2 is formed below 1270 K whereas a stable form of pure silica layer (comparable to Si-oxidized SiO_2 [14]) is formed upon annealing at 1270 K and above.

Table 2: Binding energies (BE) of different chemical species after peak decomposition of XPS C 1s spectra.

Samples	Binding energies (eV) (chemical species)
As received	282 (SiC), 285 (C-C contamination)
770 K - 30 min	282 (SiC), 282.6 (SiC_xO_y), 285 (C-C contamination)
970 K - 30 min	282 (SiC), 282.6 (SiC-oxidized SiO_2), 285 (C-C contamination)
1070 K - 30 min	282 (SiC), 282.5 (SiC-oxidized SiO_2), 285 (C-C contamination)
1270 K - 30 min	282 (SiC), 285 (C-C contamination)
1470 K - 2 h	285 (C-C contamination)

RBS spectra are presented in Fig. 5 for a DPF sample before and after annealing at 970 K for 5 h and 1470 K for 2 h. The thicknesses of the oxide layers obtained from the RBS spectra (above 10 nm) are provided in Table 1. It should be noted that iron and vanadium additives are detected at the oxidized surfaces.

The variations of the thickness of oxide layers with annealing time and temperature are presented in Figs. 6 and 7. As expected from general oxide formation kinetics [11], the thickness increases faster with temperature than with annealing time, indicating that the former parameter is the most crucial for the formation of a thick oxide layer.

Finally, a weight gain of 0.3 % is observed for the sample annealed at 1370 K for 1 h, which shows that the oxide layers detected on the SiC surfaces are formed in a passive oxidation regime.

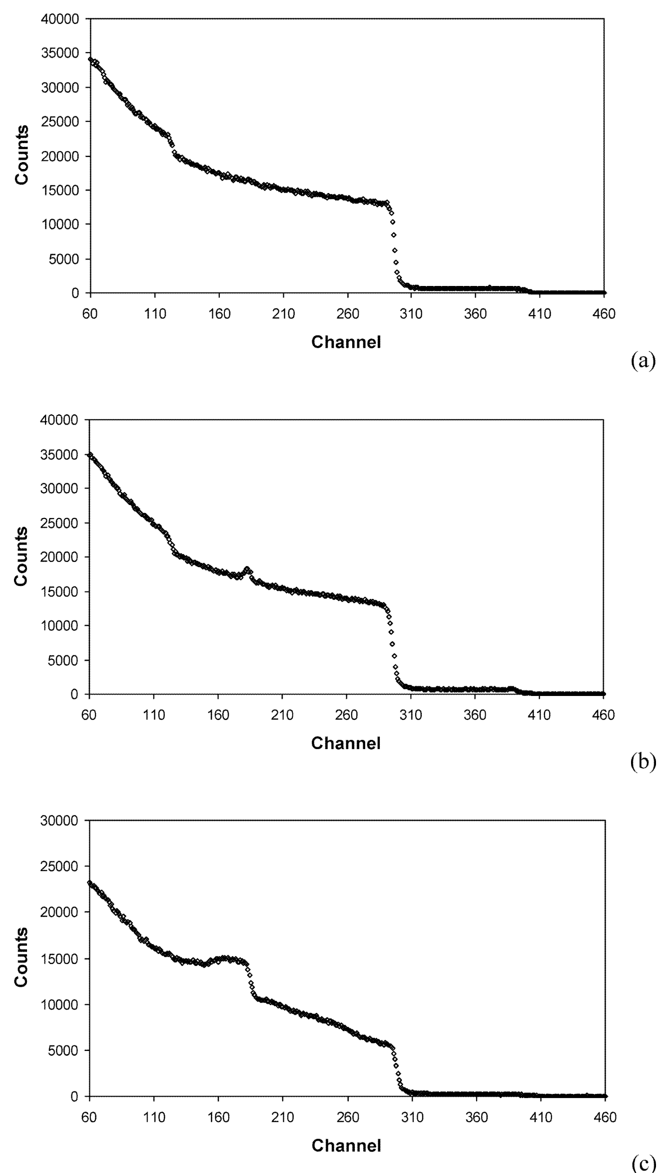

Fig. 5: RBS spectra of a DPF sample before (a) and after annealing at 970 K for 5 h (b) and 1470 K for 2 h (c).

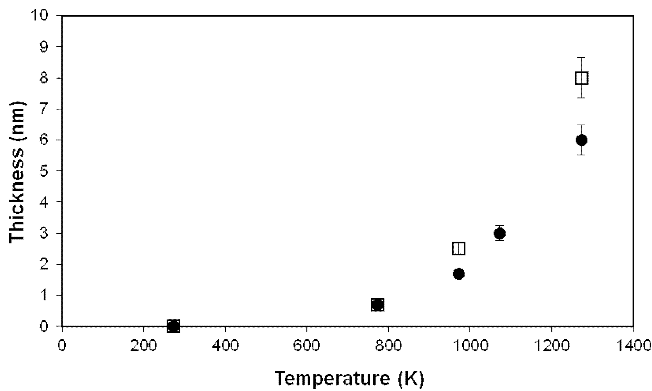

Fig. 6: Thickness of oxide layers *versus* annealing temperature. Full circles: 30 min annealing; open squares: 2 h annealing.

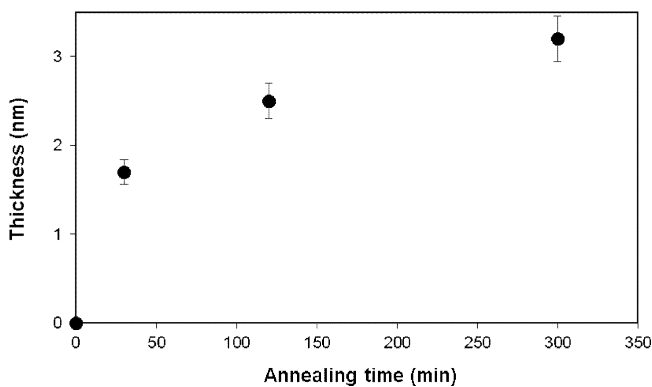

Fig. 7: Thickness of oxide layers *versus* annealing time at 970 K.

IV. Conclusion

The silicon carbide walls of an as-received DPF sample (before annealing) do not exhibit the presence of a SiO_2 layer. A silicon oxycarbide (SiC_xO_y) layer with a thickness of a few angstroms is first formed on the SiC surface of filters (main oxide detected for annealing temperatures up to 770 K). A layer of silicon dioxide (SiO_2) appears upon annealing between 770 and 970 K on the SiC/SiC_xO_y surface and its thickness increases with annealing time and temperature, this latter parameter being the most crucial for the oxide layer thickness increase and its composition. Two types of SiO_2 layers are identified depending on the temperature. The first SiO_2 contains carbon and can be called SiC-oxidized SiO_2 whereas the stable form of SiO_2 layer that appears upon annealing at 1270 K for 30 min and above is carbon-free and comparable to Si-oxidized SiO_2. No surface structural change occurs up to 1470 K. The SiO_2 layers are formed under a passive oxidation regime according to the weight gain observed at 1370 K. As the oxide layer formation rate is much higher at these temperatures, a temperature between 1370 and 1470 K during a relatively short time may be chosen to perform the calcination process in order to form a thick stable silica layer on the SiC DPF walls. Another issue will be to evaluate the efficiency of this silica layer in resisting active oxidation under all the different extreme conditions that can occur during the regeneration cycle in a diesel particulate filter.

References

1. Uchida, Y., Ichikawa, S., Harada, T., Hamanaka, T.: Durability study on Si-SiC material for DPF, SAE, paper 2003 – 01 – 0384, (2003).
2. Futatsuki, T., Oe, T., Aoki, H., Komatsu, N., Kimura, C., Sugino, T.: Low-temperature oxidation of SiC surfaces by supercritical water oxidation, *Appl. Surf. Sci.*, **256**, 6512, (2010).
3. Eck, J., Balat-Pichelin, M., Charpentier, L., Beche, E., Audubert, F.: Behavior of SiC at high temperature under helium with low oxygen partial pressure, *J. Eur. Ceram. Soc.*, **28**, 2995, (2008).
4. Vickridge, I.C., Trimaille, I., Ganem, J.J., Rigo, S., Radtke, C., Baumvol, I.J.R., Stedile, F.C.: Limiting step involved in the thermal growth of silicon oxide films on silicon carbide, *Phys. Rev. Lett.*, **89**, [25], 256102, (2002).
5. Charpentier, L., Balat-Pichelin, M., Audubert, F.: High-temperature oxidation of SiC under helium with low-pressure oxygen, *J. Eur. Ceram. Soc.*, **30**, 2653, (2010).
6. Das, D., Farjas, F, Roura, P.: Passive-oxidation kinetics of SiC microparticles, *J. Am. Ceram. Soc.*, **87**, [7], 1301, (2004).
7. Guerfi, K., Lagerge, S., Meziani, M.J., Nedellec, Y., Chauveteau, G.: Influence of the oxidation on the surface properties of silicon carbide, *Thermochim. Acta*, **434**, 140, (2005).
8. Mayer, M.: SIMNRA, a simulation program for the analysis of NRA, RBS and ERDA, in: Duggan, J.L., Morgan I.L. (Eds.), Proc. 15th Int. Conf. Appl. Accelerators in Research and Industry, AIP Conf. Proc., **475**, 541, (1999).
9. Shirley, D.A.: High-resolution X-ray photoemission spectrum of the valence bands of gold, *Phys. Rev.*, **B5**, 4709, (1972).
10. Soukiassian, P., Amy, F.: Silicon carbide surface oxidation and SiO_2/SiC interface formation investigated by soft X-ray synchrotron radiation, *J. Electron. Spectrosc.*, **144**, 783, (2005).
11. Wittberg, T.N., Wang P.S., Hsu, S.M.: Surface oxidation kinetics of SiC powders in wet and dry air studied by X-ray photoelectron spectroscopy, *Surf. Interf. Anal.*, **35**, 773, (2003).
12. Wang, J., Zhang, L., Zeng, Q., Vignoles, G.L., Guette, A.: First principles investigation on the initial stage of 2H-SiC(001) surface oxidation, *J. Am. Ceram. Soc.*, **91**, [5], 1665, (2008).
13. Song, Y., Dhar, S., Feldman, L.C., Chung, G., Williams, J.R.: Pressure dependence of SiO_2 growth kinetics and electrical properties on SiC, *J. Appl. Phys.*, **95**, 4953, (2004).
14. Kurimoto, H., Shibata, K., Kimura, C, Aoki, H., Sugino, T.: Thermal oxidation temperature dependence of 4H-SiC MOS interface, *Appl. Surf. Sci.*, **253**, 2416, (2006).
15. Radtke, C., Brandao, R.V., Pezzi, R.P., Morais, J., Baumvol, I.J.R., Stedile, F.C.: First principles-based investigation of kinetic mechanism of SiC(0001) dry oxidation including defect generation and passivation, *Nucl. Instrum. Meth. B.*, **190**, 579, (2002).
16. Chen, X., Ning, L., Wang, Y., Li, J., Xu, X., Hu, X., Jiang, M.: Thermal oxidation of silicon carbide substrates, *J. Mater. Sci. Technol.*, **25**, [1], 115, (2009).
17. Hornetz, B., Michel, H.J., Halbritter, J.: ARXPS studies of SiO_2-SiC interfaces and oxidation of 6H SiC single crystal Si-(001) and C-(001) surfaces, *J. Mater. Res.*, **9**, 3088, (1994).
18. Lu, Z.H., McCaffrey, J.P., Brar, B.: Thickness metrology of ultra-thin gate SiO_2 films, *Appl. Phys. Lett.*, **71**, [19], 2764, (1997).
19. Seah M.P., Spencer, S.J.: Ultra-thin SiO_2 on Si: IV, Thickness linearity and intensity measurement in XPS, *Surf. Interf. Anal.*, **35**, 515, (2003).